



Research Article

Optimum design analysis of a solar-assisted LiBr/H₂O absorption system with a flat-plate collector

Rahul ROY¹, Balaram KUNDU^{1,*}

¹Department of Mechanical Engineering, Jadavpur University, Kolkata, India

ARTICLE INFO

Article history

Received: 07 June 2019

Accepted: 10 October 2019

Key words:

Absorber plate; LiBr/H₂O absorption system; Solar flat-plate collector; Operating condition; Optimisation

ABSTRACT

An analytical analysis has been presented to evaluate the performance of a solar-assisted vapour absorption cooling system with a flat-plate absorber plate. The lithium–bromide water absorption cycle is used to obtain the cooling effect. The performance parameters, namely absorber plate efficiency, collector efficiency factor, heat removal factor, etc. have been determined with the variation of collector fluid inlet temperature. The cycle coefficient of performance (COP), system COP, refrigerating efficiency of the cycle, and refrigerating efficiency of the system are determined analytically. The maximum COP and cooling efficiency for both the cycle and system has been found at an optimal collector fluid inlet temperature. The optimum design condition for the variation of different design parameters, such as ambient temperature and thermal conductivity, has also been studied. Finally, the plate material is found to be a minimum at a particular collector fluid inlet temperature which is an optimum design condition to run the solar-assisted vapour absorption system.

Cite this article as: Roy R, Kundu B. Optimum design analysis of a solar-assisted LiBr/H₂O absorption system with a flat-plate collector. J Ther Eng 2021;7(5):1056–1066.

INTRODUCTION

The utilisation of solar energy for cooling purposes is an effective solution for energy savings in residential and commercial buildings. The use of fossil fuels such as coal, oil, and gas, have led to increasing in greenhouse gases, resulting in environmental pollution and global warming. About 10% of the total energy produced, is used in commercial buildings for space heating and cooling. Due to the increase

in energy demands, it is necessary to depend on renewable sources of energy for daily needs. Solar energy is an abundant source of renewable energy, which can be harnessed to provide energy to various applications. Solar cooling systems are widely developed in areas, which have little access to electricity and have abundant sunlight throughout the year. The simplest way to use solar energy for cooling purposes is the vapour absorption refrigerant system, due to

*Corresponding author.

*E-mail address: bkundu@mech.net.in (Prof. Balaram Kundu)

Department of Mechanical Engineering, Jadavpur University

This paper was recommended for publication in revised form by Regional Editor Hatice Mercan



their easy operation and production. A number of absorption systems have been researched and developed recently, which can be powered by solar heat or waste heat generated from industrial power plants.

In solar-assisted absorption systems, a flat-plate collector is used as a heat exchanger, to receive the incident solar radiation that falls on it and convert it into the internal heat energy of the collector fluid. The thermal energy of the collector fluid is used to heat the absorbent/refrigerant solution in the generator. The resultant refrigerant vapour is condensed in a condenser and transferred to the evaporator through a throttling device. The cooling occurs in the evaporator as the refrigerant evaporates at a low temperature. The refrigerant vapour mixes with the weak refrigerant solution in the absorber to form a rich aqueous refrigerant solution, which passes to the generator through a pump and a heat exchanger. The low-pressure vapour of the evaporator is delivered to high pressure in the condenser by the combined action of the generator, collector, and absorber system. The performance of the solar-assisted cooling system depends both on the collector and vapour absorption system. The flat-plate collector is an important part of the solar cooling system to generate low-grade heat energy. The absorber plate in the solar collector is responsible for the conversion of solar heat to the thermal energy of the collector fluid. A number of flat-plate collectors having different profiles have been designed to optimise their performance and increase the thermal conductivity of the absorber plate. A divergent profile shape of the absorber plate is necessary to increase the heat transfer rate from the plate to the fluid. So, a concave parabolic profile of the plate has a maximum heat energy transfer rate than the other profiles having similar volumes [1]. But due to its complex profile, it is very difficult and expensive to fabricate this typical geometry on a large scale. A triangular profile has a similar heat transfer rate to the parabolic profile, but it is impractical to manufacture it due to its zero tip thickness. Therefore, a trapezoidal profile with a small tip thickness is possible to fabricate with the least material. The easiest profile to manufacture is the rectangular profile and is widely used in flat-plate collectors. Hollands and Stedman [2] developed a step-fin flat-plate collector (SFC) to reduce the material and cost of the collector. Their work was modified to find the optimum fin dimensions of the step-fin rectangular flat-plate collector by Kundu [3]. It was found that SFC has a better heat transfer rate per unit volume compared to a rectangular-fin flat-plate collector (RFC). A new profile shape named a recto-trapezoidal profile was developed by Kundu [4]. The thermal analysis and performance optimisation of the recto-trapezoidal profile collector (RTC) was carried out with different geometric parameters. It was found that the fin efficiency of RTC was comparable to triangular profile absorber plate but lower than RFC. But, RTC is better than other profile shapes to transfer more energy at the identical absorber plate volume.

A generalised method to design a flat-plate collector was developed by Kowalski and Foster [5] based on the solar collector theory. This method was developed based on the heat transfer characteristics of the solar collector rather than its optical properties. Numerous studies have been conducted to develop a better solar absorption cooling cycle by using different refrigerants such as ammonia-water, LiBr-water, and ammonia-sodium thiocyanate. Hattem and Dato [6] designed a solar cooling system with the LiBr-H₂O absorption cycle. The overall system efficiency of the cooling system was found to be 11% during the whole season. Similar results were obtained during field-testing of a solar energised cooling system by Syed et al. [7]. It was concluded that the cooling system works best in a dry and hot climates with changing relative humidity and dry bulb temperature. Li and Sumathy [8] modified the absorption system by partitioning a single storage tank into two parts to achieve a higher coefficient of performance. The analysis of the LiBr-H₂O absorption cycle was done by Florides et al. [9] to solve the heat and mass transfer equations of the working fluid with the help of a computer program. The general design guidelines of an absorber operating at optimum conditions in a LiBr-H₂O absorption cycle has been presented by Andberg and Vliet [10]. For the simplicity of design and fabrication, RFC has been widely used in practical applications [11]. A comprehensive study on the LiBr-H₂O absorption cycle had been presented by Somesh et al. [12].

The results of the performance parameters and the thermal analysis of RFC collectors were determined by Kundu [3]. As the solar energy absorbed by the collector plates are used to operate the vapour absorption refrigeration cycle, it was necessary to do a combined analysis on both the systems considered together. Kundu [13] studied the overall system performance of the combined collector and absorption cooling cycle of an SFC. The results showed that there was a significant impact of the collector fluid inlet temperature on the overall performance parameters of the combined system. As RFC is significantly easier to manufacture than SFC, it is widely used in practice. Recently a review paper on vapour absorption systems working on LiBr/H₂O was written by Karimi et al. [14]. Furthermore, the cover material of the flat-plate solar collector and its thickness significantly affects the heat transfer rate through the absorber plate [15–17]. Its performance can be further enhanced with nanotechnology [18, 19].

From the above literature, it is obvious that the researchers have rarely concentrated on solar-assisted vapour absorption cooling system using a simple absorber plate-like RFC to determine the minimum area required to run the system with the variation of collector fluid inlet temperature under a constant cooling load application in Mumbai, India. It has been motivated to carry out the present work. The present study is based on the combined analysis of the rectangular flat-plate solar collector and the vapour absorption cycle to obtain the overall system performance and the optimum

design condition. The thermal analysis of the LiBr-H₂O absorption cycle using RFC was used to determine various system performance factors with the variation in collector fluid inlet temperature $T_{f,i}$. A mathematical model was developed to find the collector performance factors such as fin efficiency, collector efficiency factor, collector flow factor, heat removal factor, and the instantaneous collector efficiency. A simulation technique is used with the variation of collector fluid inlet temperature to determine the optimal $T_{f,i}$ at which the maximum coefficient of performance (COP) and the cooling efficiency of the cycle and system occurred. The heat transfer rate in various components of the absorption cycle has also been determined. The optimal $T_{f,i}$ to have a minimum absorber plate surface area and plate volume has been calculated for achieving the same cooling effect. The effect of ambient temperature and thermal conductivity of the material on the plate volume has also been studied in the present analysis.

MATHEMATICAL ANALYSIS

Figure 1 shows the schematic of the H₂O/LiBr absorption cooling system coupled with a flat-plate collector [19]. A rectangular flat-plate collector (RFC) is used in the present H₂O/LiBr absorption cooling system to collect the solar radiation energy that falls on its surface and converts it into thermal energy of the transport medium. A collector fluid-carrying tube is attached below the absorber plate. The base temperature of the absorber plate at the tube bond T_b is taken constantly. The hot collector fluid is supplied to the generator to heat the LiBr-H₂O solution to separate out water vapour. The water vapour acts as the refrigerant in the vapour absorption cycle and gets cooled in the condenser. It is then passed to the evaporator through an expansion valve, which takes heat from the cooling space to get evaporated at a lower pressure. The strong solution left in the generator passes through

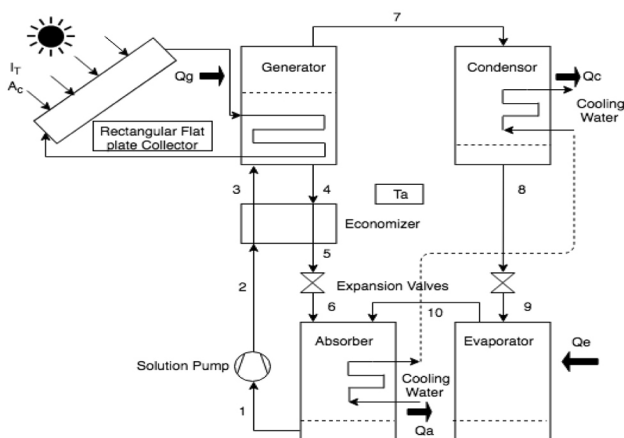


Figure 1. Flow diagram for solar-assisted single stage H₂O/LiBr vapour absorption refrigeration system.

the economizer to preheat the rich aqueous solution entering the generator. The strong solution mixes with the refrigerant from the evaporator in the absorber. The resultant aqueous solution is cooled with the help of cooling water from the cooling tower to remove the heat by mixing and absorption processes. The cooling water is reused in the condenser to cool the refrigerant. The rich aqueous solution is pumped through a drain heat exchanger and an economizer to the generator where it again gets heated by the collector fluid.

An absorber plate with the rectangular profile is shown in Figure 2. The geometrical construction of the collector plate is symmetric and repetitive about the collector fluid-carrying tube. Hence, only a part of the collector plate is presented in the figure. For the present analysis of the collector, the following assumptions are made:

- The conduction of heat energy occurs at a one-dimensional steady-state.
- The surrounding ambient temperature is uniform.
- The absorber plate material is homogenous, uniform and has constant thermal conductivity.
- The base temperature of the absorber plate is taken constantly.
- The width of the absorber plate is taken as unity.
- The incident radiation from the sun that falls on the absorber plate is taken constantly.
- The overall loss coefficient is taken to be uniform over the surface area of the plate.

Kundu [3] has already determined the temperature distribution in RFC along the length of the absorber plate. Due to the symmetric geometric construction, there is no resultant heat transfer at the midsection of the absorber plate. Hence, the maximum plate temperature occurs at the middle of the two tubes. An energy balance on a differential element of an RFC gives the governing equations for the temperature distribution. The temperature distribution depends on the two parameters, the incident flux absorbed by the absorber plate (I_a) and the overall loss coefficient (U_c). Duffie and Beckman [20] and Kundu [13] had given the necessary equation to determine the values of the two parameters, which depend upon the geographical location,

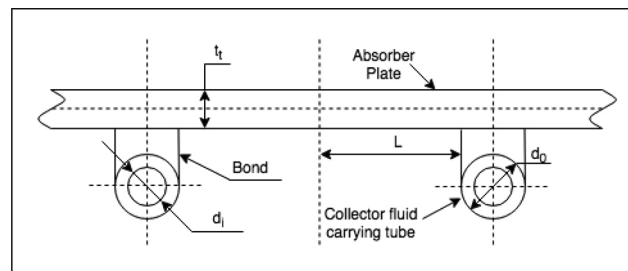


Figure 2. Schematic 1-D view of a rectangular flat-plate collector.

time, and orientation of the absorber plate. The values of I_a and U_c are given by the following equations:

$$I_a = I_b R_b (\tau\alpha)_b + I_d \left(\frac{1 + \cos\beta}{2} \right) (\tau\alpha)_d + I\rho_g \left(\frac{1 - \cos\beta}{2} \right) (\tau\alpha)_g \quad (1)$$

and

$$U_c = U_t + U_b + U_e \quad (2)$$

The fin efficiency for RFC [3] is given by

$$\eta = \tanh(Z_0)/Z_0; Z_0 = \sqrt{Bi}/\phi; Bi = U_c t_c/k_c; \phi = t_c/L \quad (3)$$

The total energy transfer rate in the absorber plate per unit width is given by

$$Q = \frac{q}{k_c(T_b - T_a - I_a/U_c)} = \phi Z_0 \tanh(Z_0) \quad (4)$$

The solar energy that is absorbed by the absorber plate is transferred through the rectangular plate to the region above the collector fluid-carrying tube. Then, the useful heat is transferred from the tube bond to the collector fluid. The useful heat gain in the direction of collector fluid per unit width is calculated as

$$q_U = -k_c F' (T_{f,i} - T_a - I_a/U_c) (2\phi Z_0^2 + Bi\mu/\phi) \quad (5)$$

The collector efficiency factor F' is given by

$$F' = \left[\frac{2\phi Z_0^2 + Bi\mu/\phi}{2\phi\eta Z_0^2 + Bi\mu/\phi} + k_c (2\phi Z_0^2 + Bi\mu/\phi) \left\{ \frac{1}{k_{bond}} + \frac{\ln(d_o/d_i)}{2\pi k_t} + \frac{1}{\pi h_i d_i} \right\} \right]^{-1} \quad (6)$$

As the thermal energy is conducted from the bond to the collector fluid, the temperature increases as the fluid flow from the inlet to the outlet of the tube. The increase in temperature in the direction of the flow can be expressed as

$$\phi = \frac{T_a - T_{f,i}}{I_a/U_c + T_a - T_{f,i}} = 1 - \exp\left(-\frac{A_c U_c F'}{\dot{m}_w c_{pw}}\right) \quad (7)$$

The total useful energy gain by the collector fluid is expressed in terms of surface area of the absorber plate A_c and heat removal factor of the collector F_R as

$$q_{UT} = F_R A_c \left[I_a - U_c (T_{f,i} - T_a) \right]; A_c = nWL(\mu + 2); F_R = \dot{m}_w c_{pw} \phi / A_c U_c \quad (8)$$

Eq. (8) can be applied to any flat-plate collector to determine the useful heat gain q_{UT} by the collector as the function of fluid inlet temperature. The hear removal factor F_R is defined as the ratio of the actual useful heat gain by the collector to the useful heat gain if the whole collector is at collector fluid inlet temperature. F_R is used to reduce the solar heat gain by taking into consideration of the mass flow rate of the collector fluid and the losses that occur in the collector U_c . The collector flow factor F'' is the ratio of the heat removal factor to the collector efficiency factor F' as given by

$$F'' = \frac{F_R}{F'} = \frac{\dot{m}_w c_{pw}}{A_c U_c F'} \left[1 - \exp\left(-\frac{A_c U_c F'}{\dot{m}_w c_{pw}}\right) \right] \quad (9)$$

It can be seen from Eq. (9) that the collector flow factor is the function of dimensionless collector capacitance rate. As the mass flow rate increases, the heat removal factor F_R increases correspondingly, and the temperature rise throughout the collector decreases. This leads to an increase in the useful heat gain in the collector q_{UT} . Hence, the collector flow factor F'' is an important parameter to determine the change in q_{UT} with respect to the mass flow rate of the collector fluid. The temperature of the absorber plate remains high compared to the fluid temperature. The mean plate temperature of the absorber plate can be determined from the following equation:

$$T_{pm} = T_{f,i} + \frac{q_{UT}(1 - F_R)}{A_c U_c F_R} \quad (10)$$

The total incident radiation on the inclined absorber plate is found by

$$I_T = I_b R_b + I_d \left(\frac{1 + \cos\beta}{2} \right) + I\rho_g \left(\frac{1 - \cos\beta}{2} \right) \quad (11)$$

From Eqs. (8) and (11), we can determine the instantaneous collector efficiency as

$$\eta_c = \frac{q_{UT}}{A_c I_T} \quad (12)$$

The dimensionless plate volume per unit width of the absorber plate is written as

$$U = \frac{U_c^2 V}{k_c^2} = Z_0 Bi^3 \quad (13)$$

Conservation of mass and energy laws are applied to all the components associated with the H₂O/LiBr absorption cooling system as shown in Fig. 1. The thermodynamic properties of the working fluid are calculated at various state points in the absorption cycle. All components are assumed to be working under steady-state conditions. The pump work is neglected and pressure changes are present only through an expansion valve. The mass and energy balance gives the following relations where h is the specific enthalpy; \dot{m} is the mass flow rate of the working fluid; \dot{Q} is the heat transfer rate in the components; x_1 and x_6 are the mass fraction of LiBr in the weak solution coming out of the absorber and strong solution from the generator, respectively.

The mass balance on the various components of the absorption cycle gives us the following equations:

$$\text{Evaporator: } \dot{m}_9 = \dot{m}_{10} \quad (14)$$

$$\text{Absorber: } \dot{m}_1 = \dot{m}_6 + \dot{m}_{10} \quad (15)$$

$$\text{Generator: } \dot{m}_2 = \dot{m}_4 + \dot{m}_7 \quad (16)$$

$$\text{Condenser: } \dot{m}_7 = \dot{m}_8 \quad (17)$$

The energy balance according to the first law of thermodynamics in the absorption refrigeration cycle gives the following set of equations:

$$\begin{bmatrix} \dot{Q}_{eva} \\ \dot{Q}_{abs} \\ \dot{Q}_{gen} \\ \dot{Q}_{con} \\ \dot{Q}_{eco} \end{bmatrix} = \begin{bmatrix} \dot{m}_{10}h_{10} - \dot{m}_9h_9 \\ \dot{m}_{10}h_{10} + \dot{m}_6h_6 - \dot{m}_1h_1 \\ \dot{m}_7h_7 + \dot{m}_4h_4 - \dot{m}_2h_2 \\ \dot{m}_7h_7 - \dot{m}_8h_8 \\ \dot{m}_2h_2 + \dot{m}_4h_4 - \dot{m}_3h_3 - \dot{m}_5h_5 \end{bmatrix} \quad (18)$$

In the absorber, the mass fractions x_1 and x_6 are the inputs to the cycle. Hence, the relation between \dot{m}_1 and \dot{m}_6 can be calculated as

$$\dot{m}_1 x_1 = \dot{m}_2 x_6 \quad (19)$$

The relations for the solution pump and the expansion valves in the cycle are obtained as

$$\text{Expansion valves: } h_5 = h_6; h_8 = h_9 \quad (20)$$

$$\text{Pump: } h_1 = h_2 \quad (21)$$

The coefficient of performance (COP) and the cooling efficiency (η_{co}) of the absorption cycle and the overall system can be expressed as

$$\begin{bmatrix} (COP)_{cyc} \\ (COP)_{sys} \\ (\eta_{co})_{cyc} \\ (\eta_{co})_{sys} \end{bmatrix} = \begin{bmatrix} \dot{Q}_e / \dot{Q}_g \\ (COP)_{cyc} \eta_c \\ (COP)_{cyc} / (COP)_{car} \\ (COP)_{sys} / (COP)_{car} \end{bmatrix} \quad (21)$$

Optimisation Analysis of Solar-Assisted H₂O/LiBr Absorption Cooling System

In the present study, water is used as the collector fluid, which carries the solar energy, absorbed by the rectangular flat-plate collector to heat the generator. Under steady-state conditions, heat gained by the generator is equal to the solar heat absorbed by the collector. The generator temperature T_g can be expressed in terms of the inlet temperature of the collector fluid $T_{f,i}$ and the generator heat transfer rate \dot{Q}_g as

$$T_g = T_{f,i} + \dot{Q}_g / \dot{m}_1 c_{ps} \epsilon_g \quad (22)$$

As the generator temperature is an implicit function, an iterative method has been adopted to determine its value. Firstly, a generator temperature is assumed to find all the state points in the absorption cycle according to Eqs. (14)–(21). The heat given to the generator is obtained from Eq. (18). The generator temperature is calculated by substituting all the parameters in Eq. (22) for a particular collector fluid inlet temperature $T_{f,i}$. This process is iterated to find the converged value of T_g . The collector loss coefficient and the solar heat gained by the collector are calculated for an assumed value of plate mean temperature and absorber plate surface area. From the obtained value of \dot{Q}_g ,

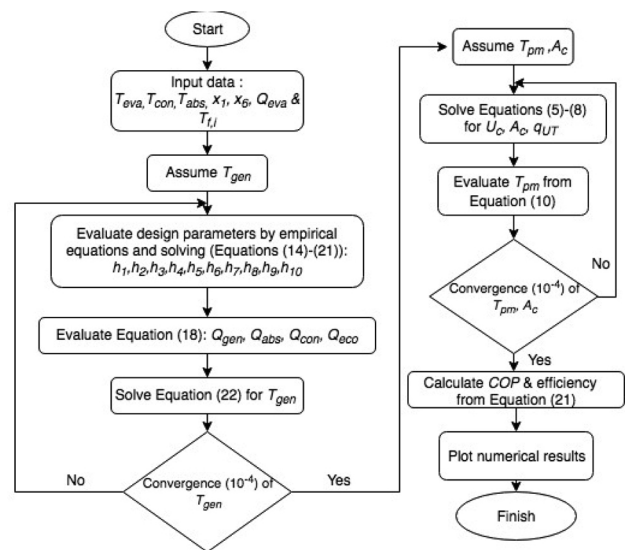


Figure 3. Flow chart for iteration to determine COP.

the plate mean temperature and absorber surface area is found from Eqs. (10) and (8), respectively. This process is repeated to obtain the converged value of T_{pm} and A_c . The absorber plate volume can be determined from Eq. (13). A flow chart for the calculation of process parameters is shown in Figure 3.

RESULTS AND DISCUSSION

Based on the above solar-assisted absorption system analysis, results have been taken for various system performance parameters as a function of the inlet temperature of the collector fluid. The above analysis can be applied to the straight rectangular profile-based flat-plate collector. The total solar radiation that falls on the collector plate is used to heat up the surface area of the plate. This heat is conducted from the collector fluid to the generator to operate the absorption cycle by boiling-off the refrigerant from the solution.

In the present study, the condenser, evaporator and absorber temperature is kept constant for a steady cooling effect. The evaporator capacity is taken as one ton of refrigeration. The generator temperature is the only variable value, which depends upon the inlet collector fluid temperature. The generator acts as a counter-flow heat exchanger between the collector fluid and the H₂O/LiBr solution. The effectiveness of the generator is taken as 0.85. The data for the calculation of various system performance factors are taken for the location in Bombay, India (Latitude = 18.9° N, Longitude = 72.817° E) on January 10, 2018, at 09:00 hours (IST). The present study is relevant for any region on Earth and at any time. Eqs. (1), (2) and (11) are used to determine the values of total incident radiation I_T , absorbent incident radiation I_a and collector loss coefficient U_c from the design specifications given in Table 1. The data was taken from the book ‘Solar engineering of thermal process’ written by Duffie and Beckman [20].

Table 1. Design specifications for solar flat-plate collector [20]

Specifications	Symbol	Value
Collector tilt angle	β	45°
Ambient temperature	T_a	27°C
Collector plate emittance	ϵ_p	0.95
Glass cover emittance	ϵ_g	0.88
Wind side heat transfer coefficient	h_w	10 W/m ² K
Ground reflectance	ρ_g	0.6
Number of glass cover	N	1
Back-insulation thickness	L_b	0.05 m
Insulation conductivity	k_b	0.045 W/mK
Edge loss coefficient of collector	U_c	0.3 W/m ² K

The design parameters to calculate enthalpy, the mass flow rate of the fluid, pressure, temperature, and mass fraction of the LiBr solution at various state points from 1 to 10 in the vapour absorption cycle are presented in Table 2. The evaporator temperature is taken above the freezing point of water as it is used as a refrigerant in the absorption cycle. Other design parameters are selected properly to obtain the heat transfer rate in various components of the single-stage LiBr/H₂O absorption cycle. The COP and the cooling efficiency are also calculated for both the cycle and the system. The operating inlet collector temperature T_{fi} for which the surface area of the absorber plate and plate volume becomes a minimum is also obtained from the present study.

For the validation of the present study, the results obtained have been compared with the existing available results in the literature. However, the results of the overall system performance factors of the RFC coupled with the LiBr-H₂O vapour absorption cooling system are unavailable as there are limited research works done in this direction. Hence, the results of the individual analysis of the two systems have been calculated and compared with the existing results. In Figure 4a, the instantaneous collector efficiency for an RFC absorber plate has been compared with the results obtained by Duffie and Beckman [20]. The variation of absorber plate inlet temperature on the cycle COP has been calculated and drawn in Figure 4b along with the previous results obtained for the vapour absorption system by Florides et al. [9]. It can be seen that the results obtained from the present model are exactly matched with the existing results.

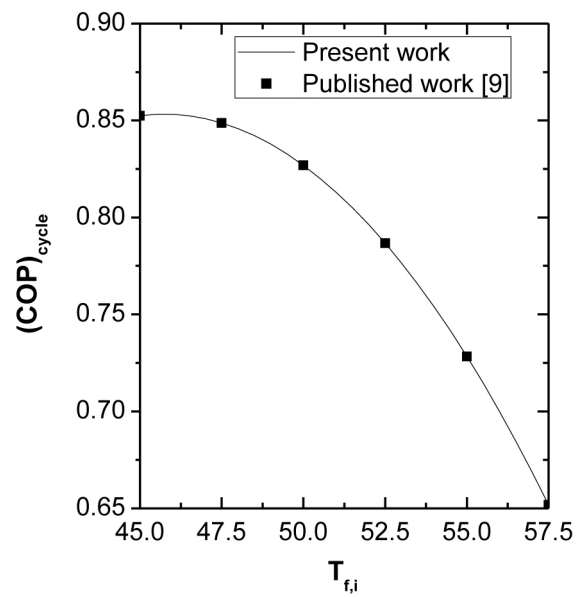
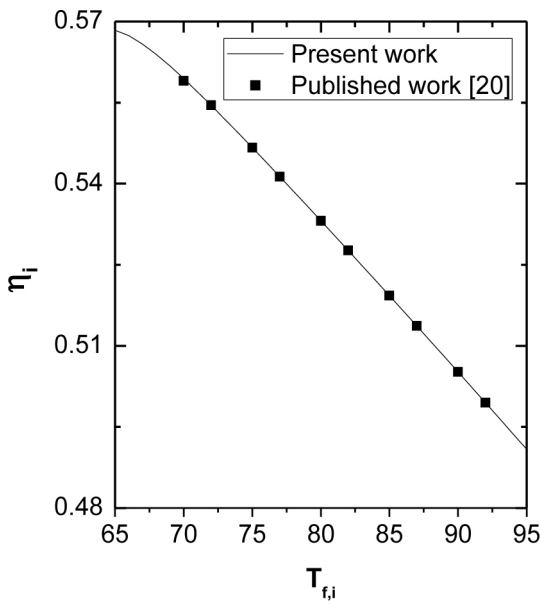
The change in the thermal performance factors of the rectangular flat-plate collector with the increase in the inlet temperature of the collector fluid is shown in Fig. 5. With the increase in T_{fi} , the overall heat loss coefficient U_c increases slightly. The fin efficiency η and collector efficiency factor F' decreases slightly, due to heat loss from the collector plate. The heat removal factor F_R depends upon the overall heat loss coefficient U_c , collector efficiency factor, and collector surface area. This change leads to a rise in

Table 2. Design parameters for H₂O/LiBr absorption cooling system [20]

Design Parameter	Symbol	Value
Evaporator Capacity	Q_e	3.51 kW
Evaporator temperature	T_{10}	6°C
Condenser temperature	T_8	45°C
Absorber temperature	T_1	26°C
Weak solution mass fraction	x_1	50% LiBr
Strong solution mass fraction	x_6	52.5% LiBr
Economizer solution exit temperature	T_3	65°C

heat removal factor F_R , reaches a maximum value at $T_{f,i} = 72^\circ\text{C}$, then decreases again with increase in $T_{f,i}$. The same trend is observed in the collector flow factor, which reaches the maximum point at $T_{f,i} = 75^\circ\text{C}$. The collector efficiency η_c decreases significantly with increase in $T_{f,i}$, due to the decrease in total solar heat gained by the collector fluid. Overall, the changes in η , F' and F_R are very insignificant with an increase in $T_{f,i}$.

Figure 6 shows the effects of $T_{f,i}$ on the heat transfer rate in various components of the vapour absorption cycle. The evaporator capacity is maintained at one ton of refrigeration at a constant temperature of 6°C . Therefore, the mass flow rate of the refrigerant is maintained at a consistent rate. As $T_{f,i}$ increases, the mass flow rate of the weak LiBr solution entering the generator decreases, leading to an increase in the generator temperature. Hence, more heat is rejected to



(a) Instantaneous collector efficiency

(b) Cycle COP vs. absorber inlet LiBr percentage ratio

Figure 4. Comparison of the results with the previous available results.

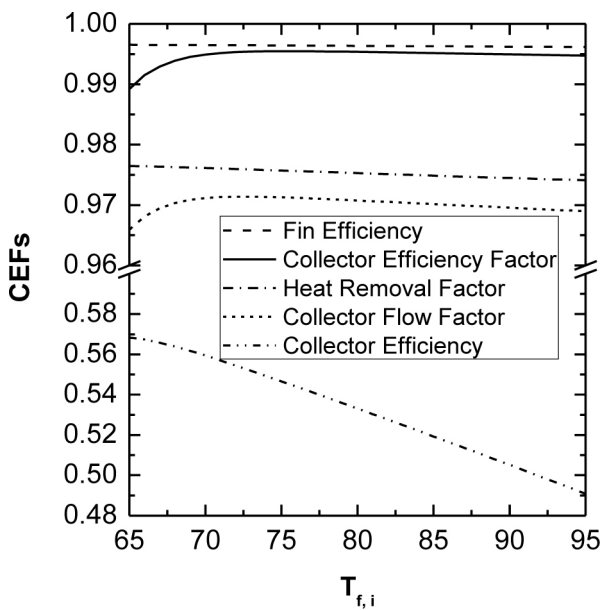


Figure 5. Collector efficiency factors as a function of $T_{f,i}$.

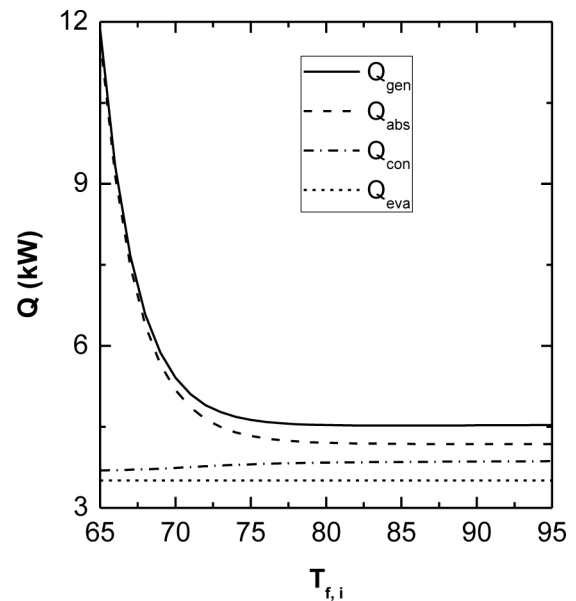


Figure 6. Heat transfer rate in different components of absorption system with variation of collector fluid inlet temperature.

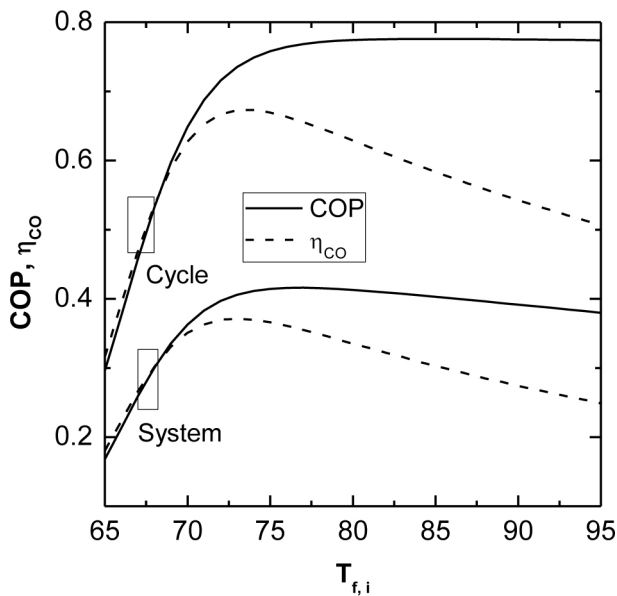


Figure 7. Coefficient of performance and cooling efficiency as a function of collector fluid inlet temperature.

the cooling water during condensation of the refrigerant to keep the condenser temperature constant. The heat transfer in the generator also decreases rapidly with the sudden decrease in the mass flow rate of the H₂O/LiBr solution. It reaches a minimum value and then increases slightly with a further increase in $T_{f,i}$. This is due to the fact that excess heat energy is required to increase the generator temperature. The optimum value of $T_{f,i}$ for which the heat transfer in the generator is minimum is the design value to have the maximum coefficient of performance of the cycle. The heat exchange rate in the absorber follows a similar trend to that of the generator. As shown in the figure, it first decreases, then reaches a minimum value, and then increases slightly.

The COP of both the cycle and the system follows a similar trend of increase to reach a maximum value for a particular $T_{f,i}$ and then decrease slightly with further increase in $T_{f,i}$. This is due to the result of a change in heat transfer rate in the generator as discussed in Figure 4. As presented in Figure 7, the COP and the cooling efficiency for the cycle is higher than the system as there is a loss of heat from the collector to the absorption cycle. The cooling efficiency reaches its maximum value faster than the COP as it depends inversely on the Carnot COP, which increases linearly with increase in $T_{f,i}$.

Figure 8 demonstrates the variation of the surface area of the rectangular flat-plate collector with increase in $T_{f,i}$. The results show that the surface area is found to have a minimum value for a particular $T_{f,i}$. At this collector inlet temperature, the overall system requires a minimum cost of the collector plate. As can be seen from the graph, there are negligible changes to the surface area when the system operates at different ambient temperatures. As the ambient

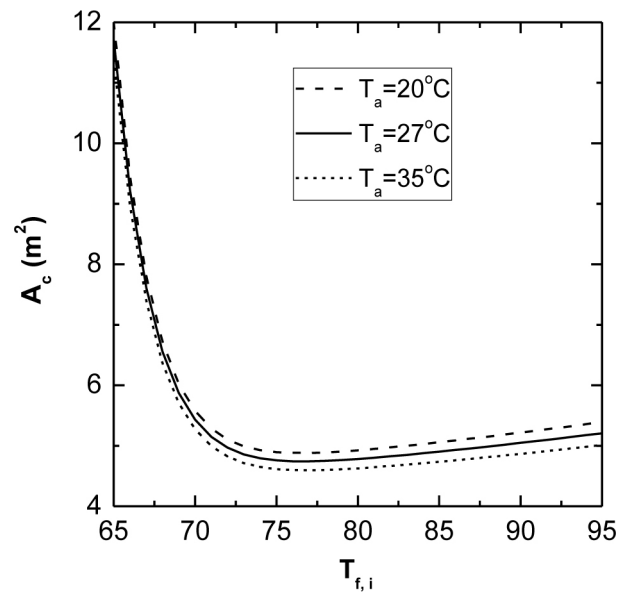


Figure 8. Influence of collector fluid inlet and ambient temperatures on collector area for the same evaporator load.

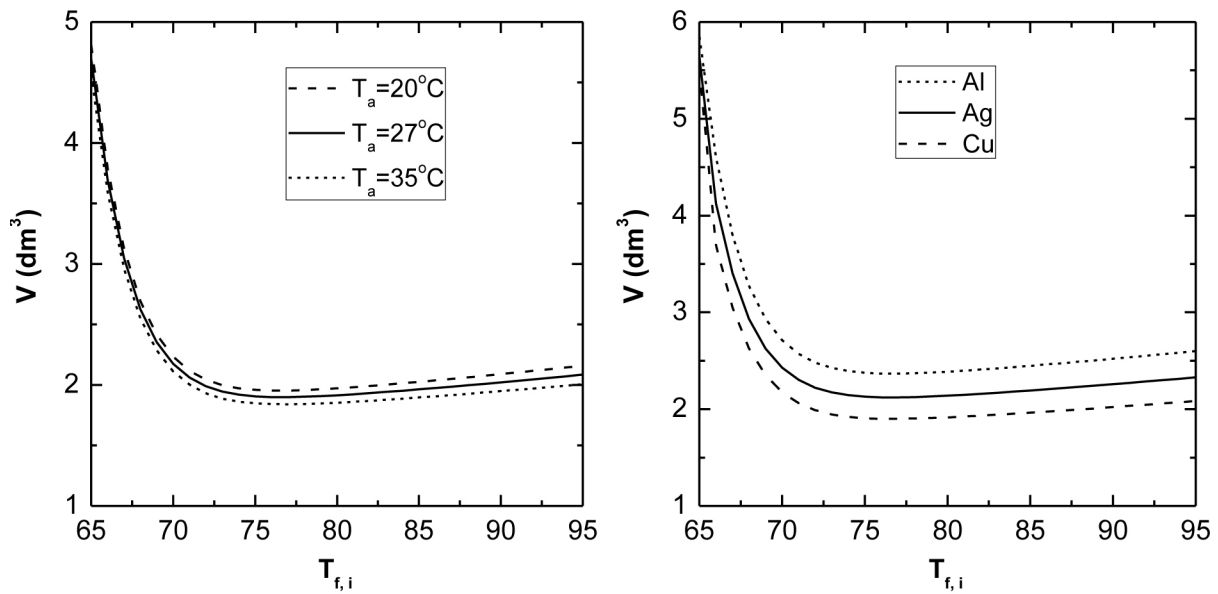
temperature decreases, more surface area of the collector is required to collect more solar heat. But, there is no change in the optimum value of $T_{f,i}$ with change in ambient temperature.

Figure 9 shows the change in plate volume of the collector plate with respect to an increase in the collector fluid inlet temperature $T_{f,i}$. It follows the same trend as found in Figure 8. The plate volume achieves a minimum value for $T_{f,i} = 77^\circ\text{C}$. Hence, it is best to operate at this optimum temperature to get minimum plate volume for the same refrigerating effect. The effect of change in ambient temperature and thermal conductivity on plate volume is shown in Figures 9a and 9b, respectively. The results show that more ambient temperature and highly conductive material are requisite for less collector plate volume.

CONCLUSION

In the present study, the thermal performance of an H₂O/LiBr absorption cooling system using a rectangular flat-plate collector has been analysed. The effect of the collector inlet fluid temperature on the system performances keeping other design parameters constant has been concluded below:

- 1 The plate efficiency and collector efficiency factor of the rectangular profile absorber plate decreases slightly with $T_{f,i}$. The solar collector efficiency also decreases with $T_{f,i}$.
- 2 The heat removal factor and the collector flow factor increase with increase in $T_{f,i}$, but fall slightly after reaching a maximum value.



(a) different ambient temperatures

(b) different plate materials

Figure 9. Design conditions for collector fluid temperature with variation of ambient temperature and different plate materials.

- The coefficient of performance and the cooling efficiency of the cycle are higher than the system and the difference amplifies with the increase in $T_{f,i}$.
- The heat transfer rates of the generator and the absorber decreases significantly with increase in $T_{f,i}$, but maintains a steady value after reaching a minimum point. The heat transfer rate in the condenser increases slightly.
- A minimum value for the surface area of the rectangular flat-plate collector has been found at $T_{f,i} = 77^\circ\text{C}$. At this temperature, the overall system requires the minimum cost of the plate. The ambient temperature of the surroundings is insignificant changes on the absorber surface area.
- A similar trend has been found for the collector plate volume. The absorber plate volume increases with a decrease in ambient temperature and thermal conductivity of the material.
- Finally, the present study helps a designer to establish a design condition of solar-assisted vapour absorption refrigeration system to run the system economically under a given cooling load at the evaporator.

NOMENCLATURE

A_c absorber plate surface area, m^2
 Bi Biot number, $U_c t / k_c$
 c_{ps} specific heat of LiBr/ H_2O solution at constant pressure, $\text{kJ}/\text{kg K}$

c_{pw} specific heat of collector fluid at constant pressure, $\text{kJ}/\text{kg K}$
 COP coefficient of performance
 d_i inner diameter of collector fluid carrying tube, 0.014m
 d_o outer diameter of collector fluid carrying tube, 0.016m
 F' collector efficiency factor
 F'' collector flow factor
 FR heat removal factor
 h specific enthalpy, kJ/kg
 h_i heat transfer coefficient in the inner side of fluid carrying tube, $300 \text{ W}/\text{m}^2\text{K}$
 h_w wind side heat transfer coefficient, $\text{W}/\text{m}^2\text{K}$
 I total radiation on horizontal surface, W/m^2
 I_a incident radiation absorbed in absorber plate, W/m^2
 I_b beam radiation on absorber plate, W/m^2
 I_d diffuse radiation on absorber plate, W/m^2
 I_T total radiation on the tilted absorber plate, W/m^2
 k_b insulation thermal conductivity, W/mK
 k_{bond} thermal conductivity of bond, $50 \text{ W}/\text{mK}$
 k_c thermal conductivity of absorber plate, W/mK
 k_t thermal conductivity of collector fluid carrying tube, $100 \text{ W}/\text{mK}$
 L distance, m
 L_b back insulation thickness of the collector, m
 \dot{m}_w mass flow rate of collector fluid, $0.5 \text{ kg}/\text{s}$
 \dot{m} mass flow rate of LiBr solution, kg/s

n	number of collector fluid carrying tube
N	number of glass cover
q	heat transfer rate, W
Q	dimensionless heat transfer rate,
q_{UT}	total useful heat gain rate per unit length, W/m
R_b	ratio of beam on tilted surface to horizontal surface
T_a	ambient temperature, °C
T_b	Tube bond temperature, °C
T_{fi}	collector fluid inlet temperature, °C
T_{fo}	collector fluid outlet temperature, °C
T_{pm}	average collector temperature, °C
t_t	absorber plate thickness, m
U	dimensionless absorber plate volume
U_b	bottom loss coefficient of the collector, W/m ² K
U_c	overall loss coefficient, W/m ² K
U_e	edge loss coefficient of the collector, W/m ² K
U_t	top loss coefficient, W/m ² K
$(UA)_{edge}$	edge loss coefficient-area product, W/K
V	absorber plate volume, m ³
W	width of absorber plate, 1m
x	mass fraction of LiBr in the solution
Z_o	dimensionless fin parameter, \sqrt{Bi}/ϕ

Greek letters

β	tilt angle, degree
μ	dimensionless diameter, d_o/L
σ	Stefan-Boltzmann constant, W/m ² K ⁴
φ	aspect ratio,
η	fin efficiency
η_c	collector efficiency
η_{co}	cooling efficiency
ε_{gen}	generator effectiveness
ρ_g	ground diffuse reflectivity
ϕ	dimensionless temperature defined in Eq. (7)
$(\tau\alpha)_b$	transmittance-absorptance product of beam radiation
$(\tau\alpha)_d$	transmittance-absorptance product of diffuse radiation
$(\tau\alpha)_g$	transmittance-absorptance product of ground-reflected radiation

Subscripts

eva	evaporator
abs	absorber
gen	generator
con	condenser
eco	economizer
car	carnot
cyc	cycle
sys	sytem
co	cooling

AUTHORSHIP CONTRIBUTIONS

Rahul Roy: Materials; Data; Analysis; Literature search; Writing. Balam Kundu: Concept; Supervision; Analysis; Critical revision; Physical interpretation; Writing; Proofs checking.

DATA AVAILABILITY STATEMENT

No new data were created in this study. The published publication includes all graphics collected or developed during the study.

CONFLICT OF INTEREST

The author declared no potential conflicts of interest with respect to the research, authorship, and/or publication of this article.

ETHICS

There are no ethical issues with the publication of this manuscript.

REFERENCES

- [1] Kovarik M. Optimal distribution of heat conducting material in the finned pipe solar energy collector. *Solar Energy* 1978; 21(6): 477–484. [https://doi.org/10.1016/0038-092X\(78\)90071-3](https://doi.org/10.1016/0038-092X(78)90071-3)
- [2] Hollands K.G.T., Stedman B.A. Optimization of an absorber plate fin having a step change in local thickness. *Solar Energy*. 1992; 49: 493–495. [https://doi.org/10.1016/0038-092X\(92\)90157-6](https://doi.org/10.1016/0038-092X(92)90157-6)
- [3] Kundu B. Performance analysis and optimization of absorber plates of different geometry for a flat-plate solar collector: a comparative study. *Applied Thermal Engineering* 2002; 22 (9): 999–1012. [https://doi.org/10.1016/S1359-4311\(01\)00127-2](https://doi.org/10.1016/S1359-4311(01)00127-2)
- [4] Kundu B. Performance and optimum design analysis of an absorber plate fin using recto-trapezoidal profile. *Solar Energy* 2008; 82 (1): 22–32. <https://doi.org/10.1016/j.solener.2007.05.002>
- [5] Kowalski G.J., Foster A.R. Heat exchanger theory applied to the design of water-and air-heating flat-plate solar collectors. *J. Solar Energy Engineering* 1988; 110 (2): 132–138. <https://doi.org/10.1115/1.3268243>
- [6] Hattem D.V., Data P.A. Description and performance of an active solar cooling system, using a LiBr-H₂O absorption machine. *Energy and Buildings* 1981; 3 (2): 169–196. [https://doi.org/10.1016/0378-7788\(81\)90023-2](https://doi.org/10.1016/0378-7788(81)90023-2)
- [7] Syed A., Lzquierdo M., Rodríguez P., Maidment G, Missenden J. A novel experimental investigation of

- a solar cooling system in Madrid. *Int. J. refrigeration* 2005; 28 (6): 859–871. <https://doi.org/10.1016/j.ijrefrig.2005.01.007>
- [8] Li Z.F., Sumathy K. Simulation of a solar absorption air conditioning system. *Energy Conversion and management*. 2001; 42 (3): 313–327. [https://doi.org/10.1016/S0196-8904\(00\)00057-1](https://doi.org/10.1016/S0196-8904(00)00057-1)
- [9] Florides G.A., Kalogirou SA, Tassou SA, Wrobel LC. Design and construction of a LiBr–water absorption machine. *Energy Conversion and Management* 2003; 44 (15): 2483–2508. [https://doi.org/10.1016/S0196-8904\(03\)00006-2](https://doi.org/10.1016/S0196-8904(03)00006-2)
- [10] Andberg J.W., Vliet G.C. Design guidelines for water-lithium bromide absorbers. *ASHRAE Trans.* 1983; 89 (1B).
- [11] Kundu B., Lee K.S. Fourier and non-Fourier heat conduction analysis in the absorber plates of a flat-plate solar collector. *Solar Energy* 2012; 86 (10): 3030–3039. <https://doi.org/10.1016/j.solener.2012.07.011>
- [12] Somesh, S., Shaw, S.K., Mahendru, P., Based Comprehensive Solar-Powered Review Vapour on LiBr–H₂O Absorption Refrigeration System. *Advances in Interdisciplinary Engineering* 2019; 343–353.
- [13] Kundu B. The influence of collector fluid inlet temperature on the performance of a solar-assisted absorption system using step-finned flat-plate collector. *Heat Transfer Engineering* 2007; 28 (5): 496–505. <https://doi.org/10.1080/01457630601166150>
- [14] Karimi M.N., Ahmad A., Aman S., Jamshed Khan M.D. A review paper on Vapor absorption system working on LiBr/H₂O, *International Research Journal of Engineering and Technology* 2018; 5 (5): 857–864.
- [15] Tekkalmaz M, Timuralp Ç, Sert Z. The effect of the use of different cover materials on heat transfer in flat solar collectors. *Journal of Thermal Engineering* 2020; 6(5): 829–42. <https://doi.org/10.18186/thermal.800158>
- [16] Dutta, J., Kundu B. Thermal Analysis on Variable Thickness Absorber plate fin in flat-plate solar collectors using differential transform method. *Journal of Thermal Engineering* 2020(1):157–69. <https://doi.org/10.18186/thermal.672169>
- [17] Bhowmick, A. Kundu, B. Thermo-economic optimization and comparison study of LiBr–H₂O and LiCl–H₂O working pair in absorption cooling systems based on genetic algorithm. *International Journal of Energy Research* 2020;1–17. <https://doi.org/10.1002/er.6048>
- [18] Hussein A.K., Walunj A., Kolsi L. Applications of nanotechnology to enhance the performance of the direct absorption solar collectors. *Journal of Thermal Engineering* 2016;2(1):529–40. <https://doi.org/10.18186/jte.46009>
- [19] Lazarus G., Siddharth R.O., Kunhappan D., Cephas E., Wongwises S. Heat transfer performance of silver/water nanofluid in a solar flat-plate collector. *Journal of Thermal Engineering* 2015;1(2): 104–12. <https://doi.org/10.18186/jte.29475>
- [20] Duffie JA, Beckman WA. *Solar Engineering of Thermal Process*. Wiley, New York, 1980.